ISSN 1330-3651 (Print), ISSN 1848-6339 (Online)
https://doi.org/10.17559/TV-20230908000924
Original scientific paper

Apex Feed Microstrip Printed Hybrid Dielectric Resonator Antenna for Wireless Application

Sobana SIKKANAN*, Balakrishnan SRINIVASAN, Jansirani GANAPATHY, Chaitanya BETHALA

Abstract: The paper introduces a fractal geometry utilizing an Octagonal Split Ring Resonator (SRR) hybrid DRA as its basis. The primary antenna consists of a conventional Octagonal patch, which is then scaled down by 0.5 in the first iteration and further by 0.25 in the second and then the DRA is utilized to enhance its performance. Remarkably compact at 6 × 6.2 cm, the antenna demonstrates effectiveness across frequencies of 5.1, 6.8, and 7.2 GHz notably; it maintains a gain above 3.3 dBi and directivity above 4.1 dBi in all operational bands. Analysis employing surface current and return loss substantiates the impact of the fractal design with DR. These simulations and measured results affirm the proposed antenna's suitability for robust C band wireless applications, offering promising performance in antenna parameters.

Keywords: dielectric resonator; fractal; hybrid DRA; microstrip; metamaterial; rectangular DRA; split ring resonator

1 INTRODUCTION

The researchers widely use the Dielectric Resonator Antenna (DRA) due to its excellent advantage of wider bandwidth with reasonable efficiency, low cost with very low fabrication complexity, high gain. DRA has overcome all the disadvantages of the conventional and other new printed antenna techniques due to its unique characteristics features like flexibility, very low conductor losses, and excellent radiation performance. The DRA may be of any shape. The circular, square, and rectangular shapes are widely used due to its fabrication simplicity, out of which the rectangular DRA is widely used due to its two-degree freedom. The Rectangular DRA characteristics depend on aspect ratio, and DRA can also be excited by different feeding techniques. In the current advancement of wireless technology, antenna with multiband characteristics plays a key role. A huge amount of narrow band applications such as WLAN, WIMAX, LTE, and so on are deployed. When crafting a wireless antenna, achieving physical compactness and retaining effective radiation is paramount. In modern antenna design, two additional vital factors are the incorporation of multiband and wideband properties [1, 2].

The microstrip patch antenna is a popular choice due to its cost-effectiveness in production and versatile fabrication capabilities. However, it does have shortcomings, including restricted bandwidth, diminished directivity, and reduced efficiency. Consequently, the printed antenna exhibits suboptimal performance and maintains a discreet profile. Despite these limitations, the patch integration unlocks applications in excess [3, 4], extending from wear technology to radio communication. This enhancement widens the scope of potential uses, demonstrating the patch's pivotal role in overcoming the antenna's inherent deficiencies. Through strategic implementation and design modifications, the microstrip patch antenna can find its niche in diverse technological landscapes, proving that even with its limitations, it remains a valuable component in the realm of wireless communication and connectivity solutions.

2 RELATED WORKS

Various strategies have been employed to enhance microstrip patch performance, including defective ground structures, ground slot additions, slotted patches, meandering, and metamaterial integration [5-8]. Metamaterials have garnered significant attention due to their intriguingly negative constitutive attributes, such as permeability, permittivity, and refractive index. These properties are determined by the material's structure rather than its chemical composition, offering a unique avenue for antenna refinement references [9-13].

Diverse metamaterial configurations are explored in the works, including SRR, CSRR, Ω shaped, double S-shaped, and 8-shaped resonators. By capitalizing on the space-filling and self-similar properties of fractal geometry, electromagnetic (EM) energy is efficiently radiated, leading to improved antenna performance, encompassing multi-band capabilities and bandwidth augmentation. To achieve miniaturization through effective lengthening, various fractal geometries have been introduced in the previous works. While these geometries hold promise in gain enhancement, they do present a challenge in fabrication due to their inherently space-filling nature. This complexity necessitates specialized manufacturing techniques [13-16]. Despite this drawback, their potential to significantly enhance antenna performance underscores their continued relevance in wireless communication technology research.

This paper introduces a novel solution for addressing wireless applications in the C band, encompassing WLAN, RADAR, and satellite communication operating at 5.1, 6.8, and 7.2 GHz. The proposed approach involves the utilization of a Two Eight-sided Split Ring Resonator (SRR) with DRA made up of alumina. This design incorporates a straightforward and less intricate self-repeating fractal structure. By synergizing metamaterial and fractal elements, the antenna achieves multi-band capabilities. The detailed design process for the suggested antenna is outlined in Section II, while the results of the proposed antenna are presented in Section III. Finally, the paper concludes with a summary of findings in Section IV.

3 DESIGN OF HYBRID DRA WITH FRACTAL GEOMETRY

The suggested antenna undergoes a three-stage evolution: Antenna A, Antenna B, and Antenna C. Antenna C represents the proposed fractal design, while Antenna A

is basic Octagonal single rings. Antenna B is the self-similar eight-sided SRR fractal structure. Constructed on an FR4 substrate, the antenna measures 6 × 6.4 × 0.16 cm. Fig. 1 illustrates the evolutionary process, while Fig. 2 provides a detailed view of the proposed structure, including its parameters. For a comprehensive listing of parameter values, please refer to Fig. 3.

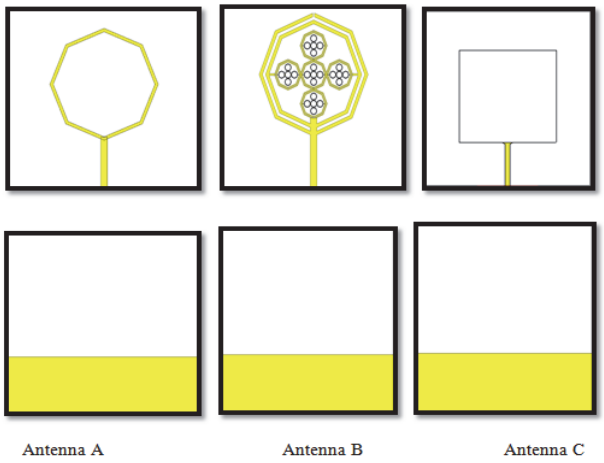

Figure 1 Proposed hybrid DRA design stages

Antenna A is a straightforward octagonal design featuring a 50-ohm microstrip feed. Its ground structure is reduced to a defective configuration. The antenna is optimized for operation within the 5 GHz frequency range. Simulated results, as depicted in Fig. 4, reveal an impressive return loss of –20.08 dB, indicating efficient performance across the frequency span of 4.25 GHz to 5.38 GHz. The VSWR analysis presented in Fig. 4 further underscores the antenna's effectiveness, with values consistently below 2 throughout the specified frequency range of 4.25 GHz to 5.38 GHz. These outcomes affirm the antenna's proficiency in transmitting and receiving signals with minimal impedance mismatch, making it well-suited for applications demanding reliable performance within the designated frequency band.

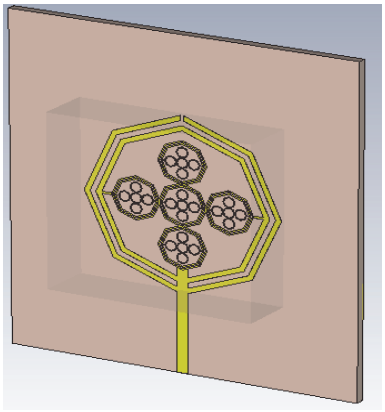

Figure 2 Proposed hybrid DRA design

In the evolution to Antenna B, first another ring is integrated and splits are introduced at opposite ends of both rings. The proposed antenna design incorporates a fractal structure, implemented in two stages. Initially, the octagonal Split Ring Resonator (SRR) is ascended down by 1/2. In the subsequent phase, the design undergoes a 1/4 scaling. The utilization of fractal structures induces a modification in surface current, leading to an increase in effective electrical length. This adjustment results in improved impedance matching [17-20]. The incorporation of the octagonal Split Ring Resonator (SRR) introduces dual-band resonance at 6.08 GHz and 5.07 GHz in the proposed antenna design. Antenna B's operational range extends from 4.601 GHz to 5.311 GHz. However, the integration of the SRR has resulted in a decrease in impedance matching. Specifically, the return loss is measured at –13.7 dB at 5.07 GHz and –12.12 dB at 6.04 GHz. This indicates that while the SRR enables dual-band resonance, it does have an impact on impedance characteristics. Detailed plots of the antenna's S11 parameter and return loss are depicted in Figs. 6 and 7, respectively. This modification to the design introduces the capability for dual-band resonance, broadening the potential applications of the antenna in various frequency ranges.

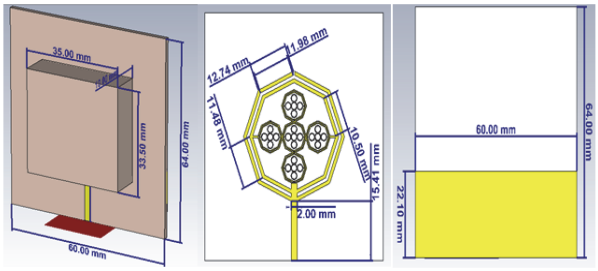

Figure 3 Hybrid DRA proposed parameter values

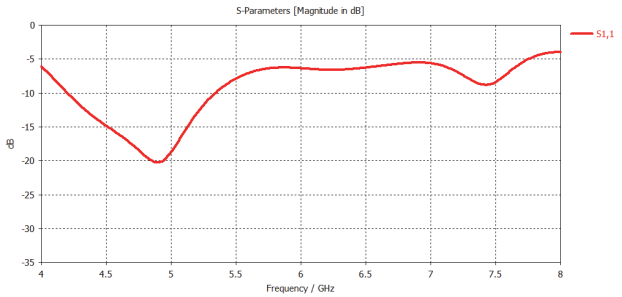

Figure 4 Return loss vs. frequency plot of antenna A

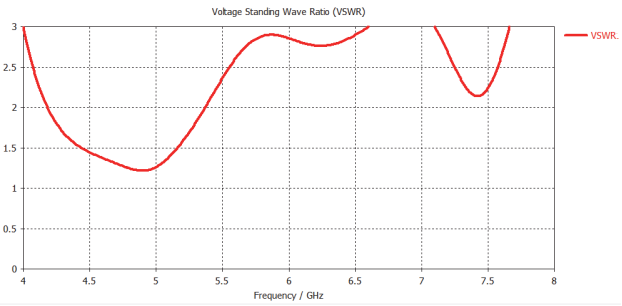

Figure 5 VSWR vs. frequency plot of antenna A

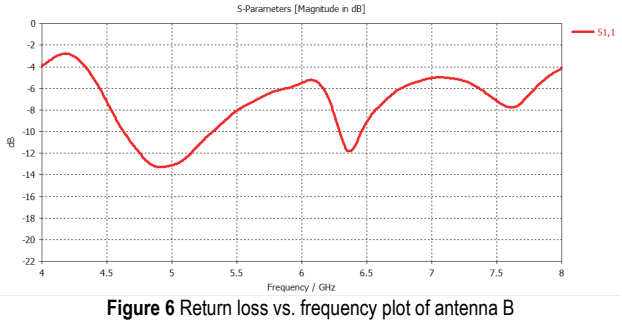

Figure 6 Return loss vs. frequency plot of antenna B

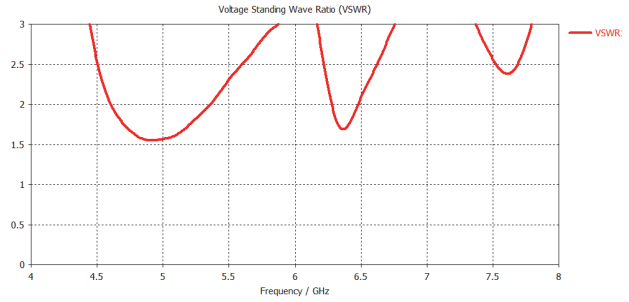

Figure 7 VSWR vs. frequency plot of antenna B

The suggested antenna demonstrates dual-band operation, resonating at 5 GHz within the frequency range of 4.695 GHz to 5.301 GHz, and also at 6.697 GHz and 6.997 GHz within the range of 6.519 GHz to 7.359 GHz. Fig. 8 provides a visual representation of the return loss for the proposed antenna. Additionally, Fig. 9 illustrates the VSWR for the antenna in operation, indicating values consistently below 2 within the specified operating bands. This confirms the antenna's efficiency in maintaining effective signal transmission and reception, validating the successful integration of fractal geometry for enhanced performance.

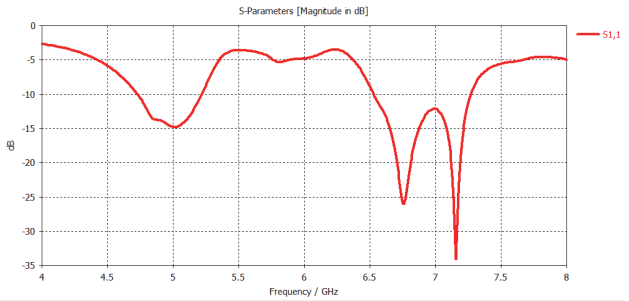

Figure 8 Return loss vs. frequency plot of antenna C

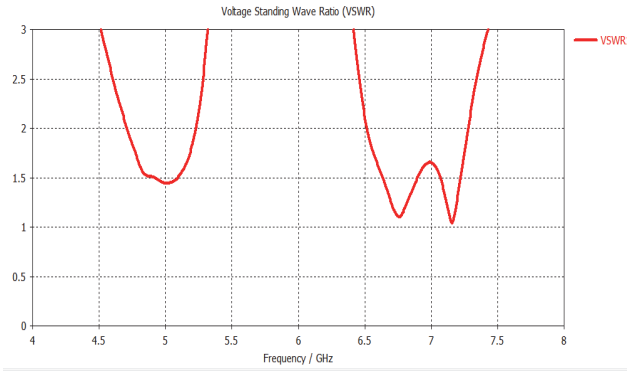

Figure 9 VSWR vs. frequency plot of antenna C

4 RESULT AND DISCUSSION

Fig. 10 presents the return loss characteristics of antennas A, B, and C. It is evident that the incorporation of metamaterial introduces dual-band resonance, and subsequently, the addition of the fractal structure further widens the bandwidth, particularly at higher frequencies.

Antenna A functions as a single-band device, with a bandwidth of 1130 MHz, covering the range from 4.25 GHz to 5.38 GHz. Upon the integration of the octagonal Split Ring Resonator (SRR), the proposed structure now operates in two bands: with the frequency range from 4.601 GHz to 5.399 GHz and,from 6.319 GHz to 6.479 GHz. The bandwidth yield at the two operating regions is of 769 MHz and 159 MHz respectively.

The introduction of fractal geometry extends the path of electrical current, leading to notable improvements in impedance characteristics and bandwidth for the proposed antenna. Consequently, the DRA introduced in the antenna now boasts bandwidth of 639 MHz and 839 MHz, effectively operating in the frequency ranges from 4.649 GHz to 5.31 GHz and, from 6.499 GHz to 7.359 GHz. This transformation signifies a substantial enhancement in the antenna's performance, showcasing the synergistic impact of both metamaterial and fractal geometry on its dual-band resonance and bandwidth capabilities.

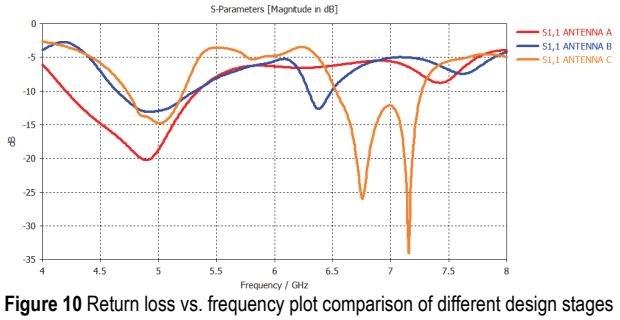

Figure 10 Return loss vs. frequency plot comparison of different design stages of the proposed antenna

At the frequency of 5 GHz, it is obvious that the majority of the surface current is focused on the outer section of the octagonal ring. This observation strongly indicates that the Split Ring Resonator (SRR) ring is primarily responsible for the 5 GHz band resonance. In Fig. 11, the distribution of surface current in proposed antenna is illustrated.

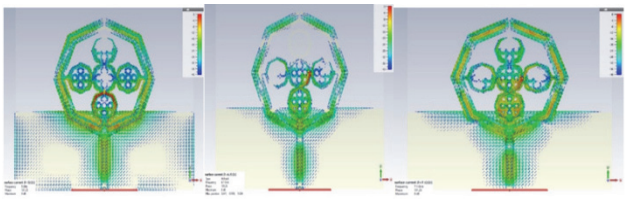

a) 5.1 GHz b) 6.8 GHz c) 7.2 GHz

Figure 11 Distribution of Surface current at various resonating frequency

Furthermore, Figs. 11b and 11c highlight the presence of surface current within the fractal structure. This observation is crucial in understanding the wideband behavior spanning from 6.52 GHz to 7.36 GHz, exhibiting dual resonance. It is explicitly attributed to the introduction of the fractal structure, as evidenced by the distribution of current.

The surface current patterns provide valuable insights into the functioning of the antenna. The dominance of surface current on the outer section of the octagonal ring at 5 GHz underscores the significance of the SRR element in achieving resonance within this frequency band. Meanwhile, the discernible presence of surface current within the fractal structure elucidates its pivotal role in enabling wideband resonance between 6.52 GHz and 7.36 GHz, showcasing the synergistic effect of the fractal structure on the antenna's dual-band performance.

Overall, these current distribution patterns serve as visual confirmation of the antenna's intricate operation and validate the design choices involving both the SRR and

fractal elements, solidifying their contributions to the antenna's dual-band resonance capabilities.

In Fig. 12, the 3D radiation pattern is presented for both the E and H planes across a range of frequencies. Notably, the antenna showcases an omnidirectional radiation pattern in the H plane, ensuring uniform signal distribution in all directions. In contrast, the E plane reveals a more intricate radiation pattern, featuring eight distinct and well-defined lobes.

Each lobe represents a specific direction of radiation, indicating the antenna's ability to focus and direct signals in a structured manner. This intricate pattern in the E plane showcases the antenna's versatility and potential for tailored signal transmission in various applications. Overall, the combination of omnidirectional radiation in the H plane and structured radiation patterns in the E plane highlights the antenna's capability to effectively cover a wide area while also providing focused and directed signal propagation when needed. This is a valuable feature for applications that require both broad coverage and targeted signal transmission. This intriguing radiation behavior is achieved through the synergistic integration of metamaterial and fractal elements, resulting in a consistently stable radiation pattern.

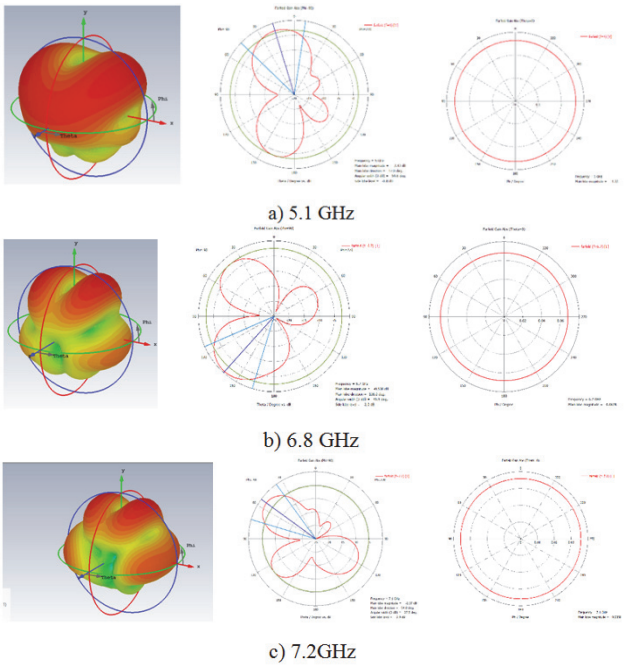

Figure 12 Radiation pattern at various resonating frequency

Table 1 Proposed DRA antenna parameters

Antenna	Centre frequency	Frequency bands	Bandwidth	Gain	Directivity
Antenna A	4.99 GHz	4.249-5.379GHz	1129 MHz	****	
Antenna B	5.01 GHz	4.61-5.38GHz	769 MHz		
	6.39 GHz	6.319-6.479GHz	159 MHz		
Antenna C	5.21 GHz	4.649-5.309GHz	639 MHz	3.499 dBi	4.599
	6.69 GHz, 7.01 GHz	6.499-7.359 GHz	839 MHz	4.889 dBi, 3.801 dBi	7.306,6.599

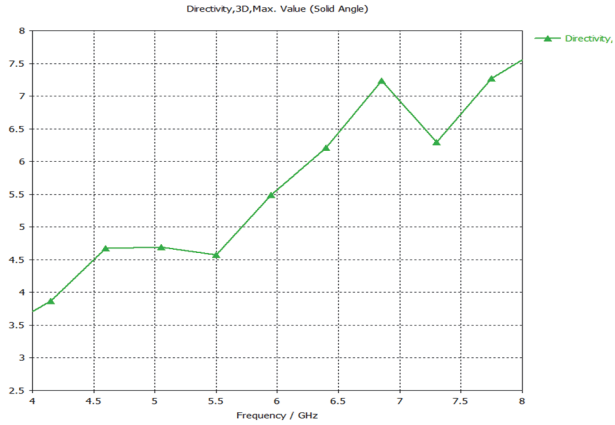

Figure 13 Hybrid DRA gain with respect to frequency

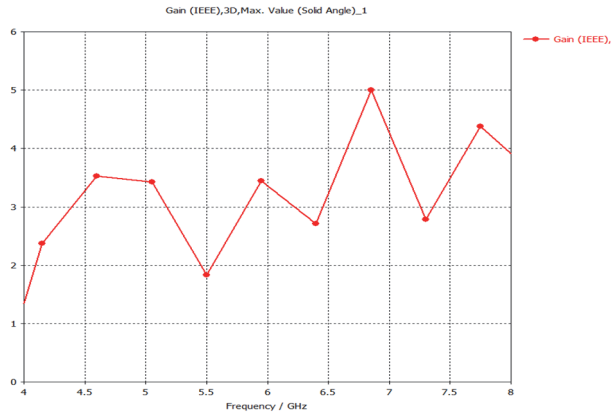

Figure 14 Hybrid DRA directivity with respect to frequency

Fig. 13 provides a directivity plot across frequency ranges, demonstrating that the proposed antenna maintains a directivity exceeding 4.5 dBi across all operational zones. This signifies a robust and focused radiation performance.

Furthermore, Fig. 14 showcases that the gain remains consistently above 2.5 dBi throughout all operating regions. This underscores the antenna's effectiveness in efficiently radiating electromagnetic energy, indicative of its suitability for a wide range of applications requiring reliable signal propagation.

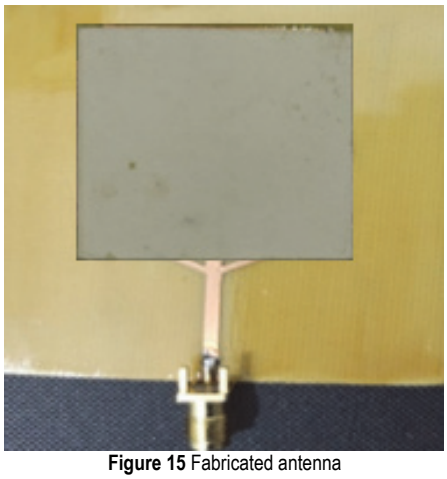

Figure 15 Fabricated antenna

The combination of metamaterial and fractal elements has evidently contributed to the antenna's superior radiation characteristics, rendering it a versatile and reliable choice for diverse wireless communication

scenarios. In Table II, the antenna parameters of the proposed DRA is presented. in Fig. 15, the fabricated antenna is presented. The proposed antenna is fabricated with the help of photolithography etching method. The comparison results between the simulated and measured is presented in Fig. 16. The deviation between the measured and simulated is due to the measurement and fabrication error.

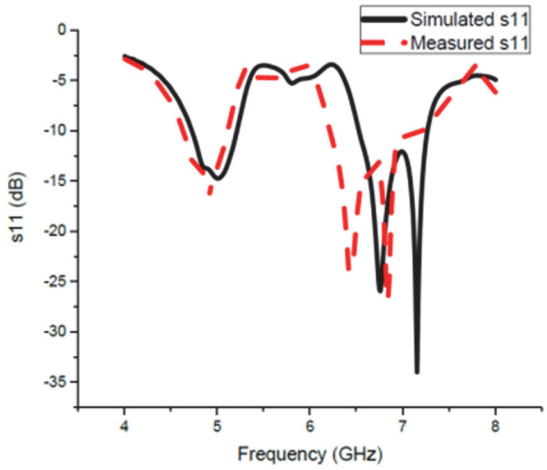

Figure 16 Simulated vs measured result

5 CONCLUSION

In conclusion, we present a novel approach for C band wireless communication through a metamaterial-based fractal antenna. Constructed on a 6cm x 6.4cm x 0.16cm FR4 substrate, the antenna undergoes a three-stage evolution. Antenna A operates from 4.249-5.379 GHz with a bandwidth of 1129 MHz Antenna B, enhanced with octagonal SRR, extends its operation from 4.61-5.38 and 6.319-6.479 GHz with respective impedance bandwidths of 769 MHz and 159 MHz Antenna C, employing fractal geometry with DRA , spans 4.649-5.309 and 6.499-7.35 GHz, with impedance bandwidths of 639 MHz and 839 MHz. The metamaterial structure enables dual-band operation, while the fractal element widens bandwidth at higher frequencies. With compact size, high gain, stable radiation pattern, and moderate directivity, this fractal antenna holds promise for applications in WLAN, RADAR, and satellite communication at 5.1, 6.8, and 7.2 GHz within the C band spectrum.

6 REFERENCES

[1] Pouyanfar, N. (2013). Broadband square slot circularly polarized antenna for WiMAX and WLAN applications. *Microwave and Optical Technology Letters*, *55*(9), 2191-2195. https://doi.org/10.1002/mop.27805

[2] Pedram, K., Nourinia, J., & Ghobadi, C. (2016). A small dual band antenna with simple structure for WLAN/WIMAX application. *International Symposium on Telecommunication (IST), Tehran, Iran*, 349-352. https://doi.org/10.1109/ISTEL.2016.7881838

[3] Li, R., Wu, C., Sun, X., Zhao, Y., & Luo, W. (2022). An EBG-Based Triple-Band Wearable Antenna for WBAN Applications. *Micromachines (Basel)*, *13*(11), 1938. https://doi.org/10.3390%2Fmi13111938

[4] Alam, T., Faruque, M. R. I., & Islam, M. T. (2015). A Double-Negative Metamaterial-Inspired Mobile Wireless Antenna for Electromagnetic Absorption Reduction. *Materials (Basel)*, *8*(8), 4817-4828. https://doi.org/10.3390/ma8084817

[5] Najumunnisa, M., Sastry, A. S. C., Madhav, B. T. P., Das, S., Hussain, N., Ali, S. S., & Aslam, M. (2022). A Metamaterial Inspired AMC Backed Dual Band Antenna for ISM and RFID Applications. *Sensors (Basel)*, *22*(20), 8065. https://doi.org/10.3390/s22208065

[6] Abolade, J. O., Konditi, D. B. O., & Dharmadhikary, V. M. (2020). Bio-inspired wideband antenna for wireless applications based on perturbation technique. *Heliyon*, *6*(7), e04282. https://doi.org/10.1016/j.heliyon.2020.e04282

[7] Afridi, A., Ullah, S., Khan, S., Ahmed, A., Khalil, A. H., & Tarar, M. A. (2013), Design of dual band wearable antenna using metamaterials. *Journal of Microwave Power and Electromagnetic Energy*, *47*(2), 126-37. https://doi.org/10.1080/08327823.2013.11689852

[8] Awan, W. A., Abbas, A., Naqvi, S. I., Elkamchouchi, D. H., Aslam, M., & Hussain, N. (2023). A Conformal Tri-Band Antenna for Flexible Devices and Body-Centric Wireless Communications. *Micromachines (Basel)*, *14*(10), 1842. https://doi.org/10.3390/mi14101842

[9] Paracha, K. N., Rahim, S. K. A., Soh, P. C., & Khalily M. (2019). Wearable antennas: A review of materials, structures, and innovative features for autonomous communication and sensing. *IEEE Access*, *7*, 56694-56712. https://doi.org/10.1109/ACCESS.2019.2909146

[10] Deng, Z., Guo, L., Chen, X., & Wu, W. (2023). Smart Wearable Systems for Health Monitoring. *Sensors*, *23*, 2479. https://doi.org/10.3390/s23052479

[11] Sowjanya, A. & Vakula, D. (2022). Compact Dual Bandpass Filter Using Dual-Split Ring Resonator for 5G Upper Microwave Flexible Use Services. *Journal of Electromagnetic Engineering and Science*, 22, 434-439. https://doi.org/10.26866/jees.2022.4.r.106

[12] Hussain, M., Ali, E. M., Awan, W. A., Hussain, N., Alibakhshikenari, M., Virdee, B. S., & Falcone, F. (2022). Electronically reconfigurable and conformal triband antenna for wireless communications systems and portable devices. *PLoS ONE*, *17*, e0276922. https://doi.org/10.1371/journal.pone.0276922

[13] Ashyap, A. Y. I., Dahlan, S. H. B., Abidin, Z. Z., Rahim, S. K. A., Majid, H. A., Alqadami, A. S. M., & Atrash, M. A. (2021). Fully fabric high impedance surface-enabled antenna for wearable medical applications. *IEEE Access*, 9, 6948-6960. https://doi.org/10.1109/ACCESS.2021.3049491

[14] Vaezi, S., Rezaei, P., & Khazaei, A. A. (2022). A miniaturized wideband wearable antenna with circular polarization for medical application. *AEU - International Journal of Electronics and Communications*, *150*, 154197. https://doi.org/10.1016/j.aeue.2022.154197

[15] Singh, H., Srivastava, K., Kumar, S., & Kanaujia, B. K. (2021). A planar dual-band antenna for ISM/Wearable applications. *Wireless Personal Communications*, *118*, 631-646.

[16] Abdulkawi, W. M., Masood, A., Nizam-Uddin, N., & Alnakhli, M. (2023). A simulation study of triband low SAR wearable antenna. *Micromachines*, *14*, 819. https://doi.org/10.3390/mi14040819

[17] Roja, G., Maheswara Venkatesh, P., & Jayasankar, T. (2023). Split Ring Resonator Inspired Dual-Band Monopole Antenna for ISM, WLAN, WIFI, and WiMAX Application. *Technical Gazette*, *30*(5), 1533-1538. https://doi.org/10.17559/TV-20230210000344

[18] Dwivedi, A. K., Narayanaswamy, N. K., Penmatsa, K. K. V., Singh, S. K., Sharma, A., & Singh, V. (2023). Circularly polarized printed dual port MIMO antenna with polarization diversity optimized by machine learning approach for 5G NR n77/n78 frequency band applications. *Scientific Reports*, *13*(1), 13994. https://doi.org/10.1038/s41598-023-41302-2

[19] Sharma, P, Tiwari, R. N., Singh, P., Kumar, P., & Kanaujia, B. K. (2022). MIMO Antennas: Design Approaches, Techniques and Applications. *Sensors (Basel)*, *22*(20), 7813. https://doi.org/10.3390/s22207813

[20] Sakli, H., Abdelhamid, C., Essid, C., & Sakli, N. (2021). Metamaterial-based antenna performance enhancement for MIMO system applications. *IEEE Access*, *9*, 38546-38556. https://doi.org/10.1109/ACCESS.2021.3063630

Contact information:

Dr. Sobana SIKKANAN, Associate Professor
(Corresponding author)
Department of Electronics and Communication Engineering,
Karpagam College of Engineering,
Coimbatore
E-mail: sobanaa@gmail.com

Mr. Balakrishnan SRINIVASAN, Assistant Professor
Department of Electronics and Communication Engineering,
Vivekanandha College of Engineering for Women,
Tiruchengode, India
E-mail: balakrishnan.srini@gmail.com

Mrs. Jansirani GANAPATHY
Department of Electrical and Electronics Engineering,
University College of Engineering (BIT Campus),
Anna University,
Tiruchirappalli, Tamil Nadu, India
E-mail: g.jansirani@rediffmail.com

Mr. Chaitanya BETHALA, Research Scholar
Department of Electrical, Electronics & Communication Engineering,
GITAM School of Technology, Hyderabad Campus,
Telangana
E-mail: bchaitanya55@gmail.com